Supporting Information

Mechanochromic, Thermoresponsive and Triboluminescent Behaviors in One Divinyl Thioxanthene Based AIE Luminogen with Variable Conformation

Nengni Xu,[#] Wenhua Xu,[#] Meng Sun[b], Yi Yuan, Xinjun Luan,*[a] Ying Wang,[c] Hui Wang*[a.]

[a]Key Laboratory of Synthetic and Natural Functional Molecule of the Ministry of Education, College of Chemistry & Materials Science, Northwest University, Xi'an, 710127, China; Email: whui210@nwu.edu.cn; xluan@nwu.edu.cn.

[b]Key Laboratory of Molecular Medicine and Biotherapy, School of Life Sciences, Beijing Institute of Technology, Beijing 100811, China;

[c]Key Laboratory of Photochemical Conversion and Optoelectronic Materials, Technical Institute of Physics and Chemistry, Chinese Academy of Sciences, Beijing, 100190, China;

Table of Contents:

A. General information:

All reactions were carried out under an argon atmosphere using standard Schlenk-Lines or glovebox (Innovative Technology). THF were dried over sodium. If not specifically mentioned, all chemicals were used as received from Sigma-Aldrich Corporation, Innochem and without further purification. Analytical thin-layer chromatography was performed with 0.25 mm coated commercial silica gel plates (TLC Silica Gel 60 F_{254}); visualization of the developed chromatogram was performed by fluorescence. Flash chromatography was performed with silica gel (300-400 mesh). Proton nuclear magnetic resonance (^{1}H NMR) data were acquired on Bruker Ascend 400 (400 MHz) spectrometer. Chemical shifts are reported in delta (δ) units, in parts per million (ppm) downfield from tetramethylsilane. Coupling constants J are quoted in Hz. Carbon-13 nuclear magnetic resonance (^{13}C NMR) data were acquired at 101 MHz on Bruker Ascend 400 spectrometer. The chemical shift references were as follows: for ^{1}H NMR spectra, Chloroform-d at 7.260 ppm, and for ^{13}C NMR spectra, Chloroform-d at 77.0 ppm. High resolution mass spectra were acquired on a Bruker Daltonics MicroTof-Q II mass spectrometer. The DSC measurements were carried out using a TA Instruments DSC 2910 thermal analyzer at a heating rate of 2 °C min^{-1}. UV-Vis spectra were determined on a Hitachi U-2900 spectrometer. Fluorescence spectra were acquired on a Hitachi F-4500 fluorescence spectrometer with a 10-mm quartz cuvette. The absolute quantum yields (ϕ_F) were determined by Edinburgh FLS-920 with an integral sphere. The transient photoluminance decay characteristics were measured using an Edinburgh Instruments FLS920 spectrometer. Powder X-ray diffraction (PXRD) studies were performed on a SHIMADZU XRD-6000 Labx diffractometer using Cu-Ka radiation (λ = 1.5418 Å) with 2θ range of 2-50°, 40 KeV, and 30 mA having a scanning rate of 0.01° s^{-1} (2θ) at room temperature. Single crystal structures were measured on a Bruker SMART APEX II CCD diffractometer with a graphite monochromated Mo Kα (λ = 0.71073 Å, at 296(2) K) or a Bruker D8 VENTURE PHOTON II diffractometer with a graphite monochromated Ga Kα (λ = 1.34138 Å, at 175(2) K) radiation. Using Olex2,[1] the structure was solved with the SHELXT[2] structure solution program using Intrinsic Phasing and refined with the SHELXL refinement package using Least Squares minimization.

B. General procedure for the preparation of TXENE

Synthetic procedures

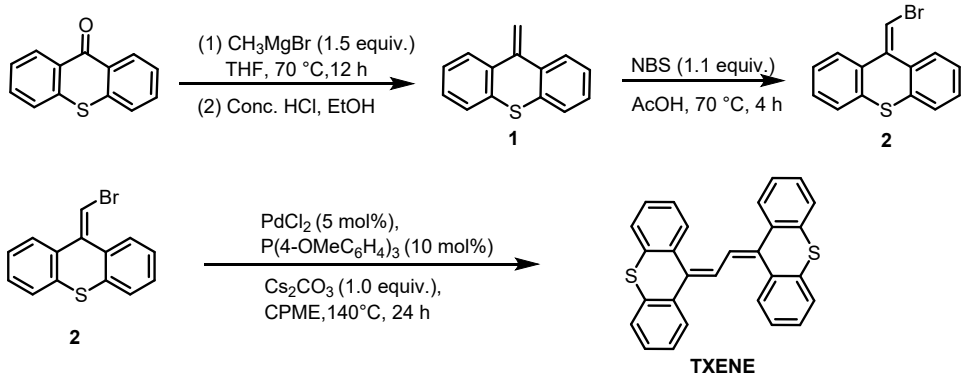

Scheme S1. Preparation of TXENE

Synthesis of 9-Methylene-9*H*-thioxanthene (1).

To a round-bottomed flask (25 ml), Thioxanthen-9-one (424.1 mg, 2 mmol) was charged under air atmosphere. After the flask was evacuated and purged with nitrogen for three times, dry THF (10.0 ml) was added by syringe. Then 3M（1 ml, 3 mmol）of methylmagnesium bromide in THF was added. The resulting mixture was stirred and reflux for 16h. After cooling, the organic phase was washed with 1M HCl three times. The solvent was evaporated under redue pressure to give an oil. To this oily residue was added 2M HCl (2ml) and stirred until TLC detected reaction over. It was extrated with saturated aq. $NaHCO_3$ and ethyl acetate three times. The organic phase was dried with anhydrous Na_2SO_4 and the solvent was removed under reduced pressure. The crude product was purified by flash silica gel column chromatography (Petroleum ether/ EtOAc = 100:1) to afford the desired product as colorless, air-sensitive oil.[3] (331.9mg，79% yield). ^{1}H NMR (400 MHz, Chloroform-d) δ 7.85 – 7.75 (m, 2H), 7.62 – 7.53 (m, 2H), 7.47 – 7.36 (m, 4H), 5.75 (s, 2H). ^{13}C NMR (101MHz, Chloroform-d) δ 142.47, 134.70, 131.44, 127.97, 126.99, 126.33, 126.14, 114.01. IR (KBr): 1577, 1483, 1342, 1316, 1256, 1147, 1105, 940, 893, 761, 741 cm^{-1}. HRMS (ESI) m/z calculated for $C_{14}H_{11}S$ $[M+H]^+$ 211.0581, found 211.0591.

Synthesis of 9-(Bromomethylene)-9*H*-thioxanthene (2).

To a suspension of **1** (210.1 mg, 1 mmol) in AcOH (5 mL) was added NBS (178.0 mg, 1.1mmol). The resulting mixture was stirred at 70 ℃ for 4 h. After cooling down to room temperature naturally, the reaction was neutralized by slowly adding NaOH/$NaHCO_3$ (1:1) and extracted with EtOAc three times. The combined organic layers were dried over $MgSO_4$ and concentrated under reduced pressure. The residue was purified by silica gel flash chromatography (petroleum ether/ EtOAc = 100:1) to afford the desired product as colorless oil. [4]（247.6mg，86% yield）。^{1}H NMR (400 MHz, Chloroform-*d*) δ 8.06 (dd, *J* = 7.5, 1.8 Hz, 1H), 7.54 (dd, *J* = 7.5, 1.6 Hz, 1H), 7.48 (ddd, *J* = 9.1, 5.7, 3.0 Hz, 2H), 7.42 – 7.30 (m, 4H), 6.74 (s, 1H).^{13}C NMR (101 MHz, Chloroform-*d*) δ 139.36, 135.94, 133.19, 132.03, 131.76, 129.16, 128.02, 127.74, 127.03, 126.70, 126.02, 125.78, 125.76, 106.29. IR (KBr): 3060, 1583, 1460, 1334, 1271, 1218, 1157, 1066, 944, 792, 735, 710, 688 cm^{-1}. HRMS (ESI) m/z calculated for $C_{14}H_{10}SBr$ $[M+H]^+$ 288.9687, found 288.9691.

Synthesis of 1,2-Di(9*H*-thioxanthen-9-ylidene)ethane (TXENE).

In a glovebox, a 5 mL vial equipped with a stirring bar was charged with 2 (57.6 mg, 0.2 mmol,), $PdCl_2$ (3.5 mg, 0.02 mmol), tris(4-methoxyphenyl) phosphine (14.1mg, 0.04mmol), cesium carbonate (130.3 mg, 0.4 mmol) followed by sequential addition of 2.0 mL anhydrous CPME. The vial was sealed with a Teflon screw cap and the reaction mixture was heated at 140 ºC for 12 h. After the reaction vessel was cooled to room temperature. After diluting with water, the reaction mixture was extrated with saturated aq. $NaHCO_3$ and ethyl acetate three times. The organic phase was dried with anhydrous Na_2SO_4 and the solvent was removed under reduced pressure. The crude product was purified by flash silica gel column chromatography (Petroleum ether) to afford the desired product as orange solid. (74.4 mg, 89% yield). ^{1}H NMR (400 MHz, Chloroform-d) δ 7.83 (dd, J = 7.7, 1.4 Hz, 2H), 7.56 (dd, J = 7.7, 1.5 Hz, 2H), 7.52 (dd, J = 7.8, 1.4 Hz, 2H), 7.47 – 7.38 (m, 4H), 7.37 – 7.31 (m, 2H), 7.31 – 7.27 (m, 2H), 7.23 (td, J = 7.5, 1.5 Hz, 2H), 7.07 (s, 2H).^{13}C NMR (101 MHz, Chloroform-d) δ 137.86, 137.62, 133.70, 133.46, 131.79, 129.82, 127.66, 127.02, 127.00, 126.91, 126.74, 125.98, 125.92, 125.29. IR (KBr): 2955, 2922, 2851, 1581, 1459, 1436, 1263, 1124, 1066, 1036, 776, 763, 737 cm^{-1}. HRMS (ESI) m/z calculated for $C_{28}H_{19}S_2$ $[M+H]^+$ 419.0928, found 419.0927.

NMR spectra

^{1}H NMR (400 MHz, Chloroform-*d*) of compound **1**:

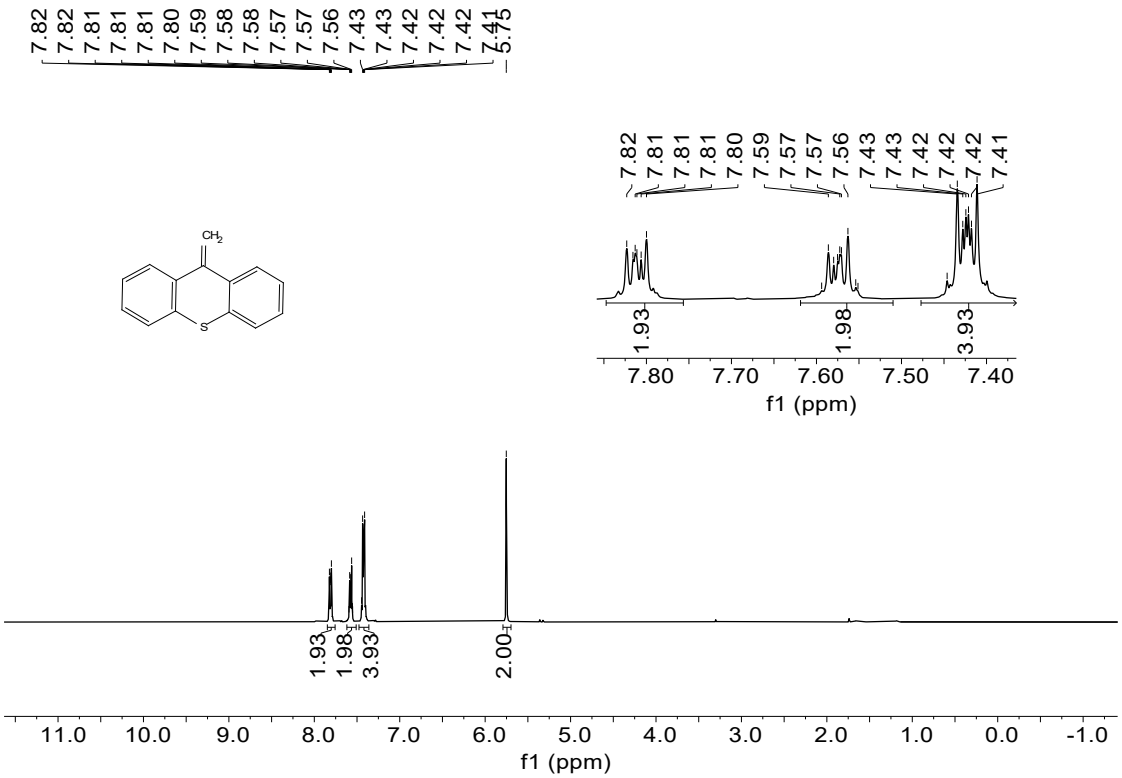

^{13}C NMR (101 MHz, Chloroform-*d*) of compound **1**:

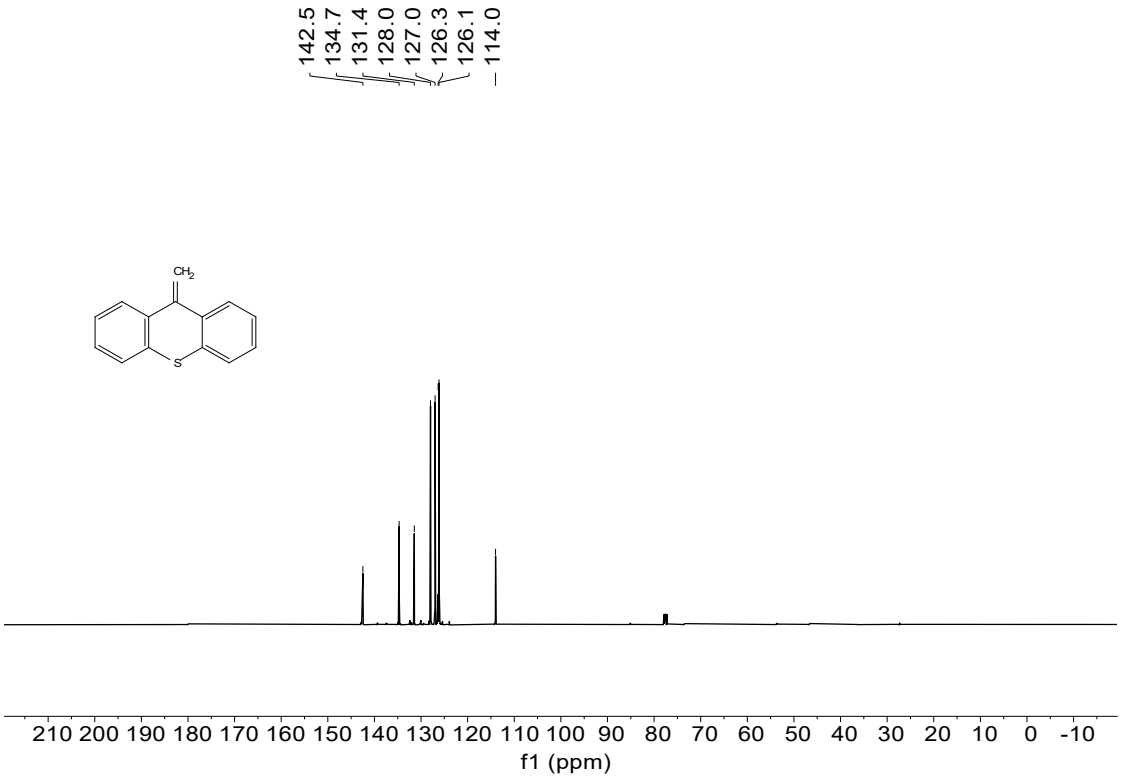

^{1}H NMR (400 MHz, Chloroform-*d*) of compound **2**:

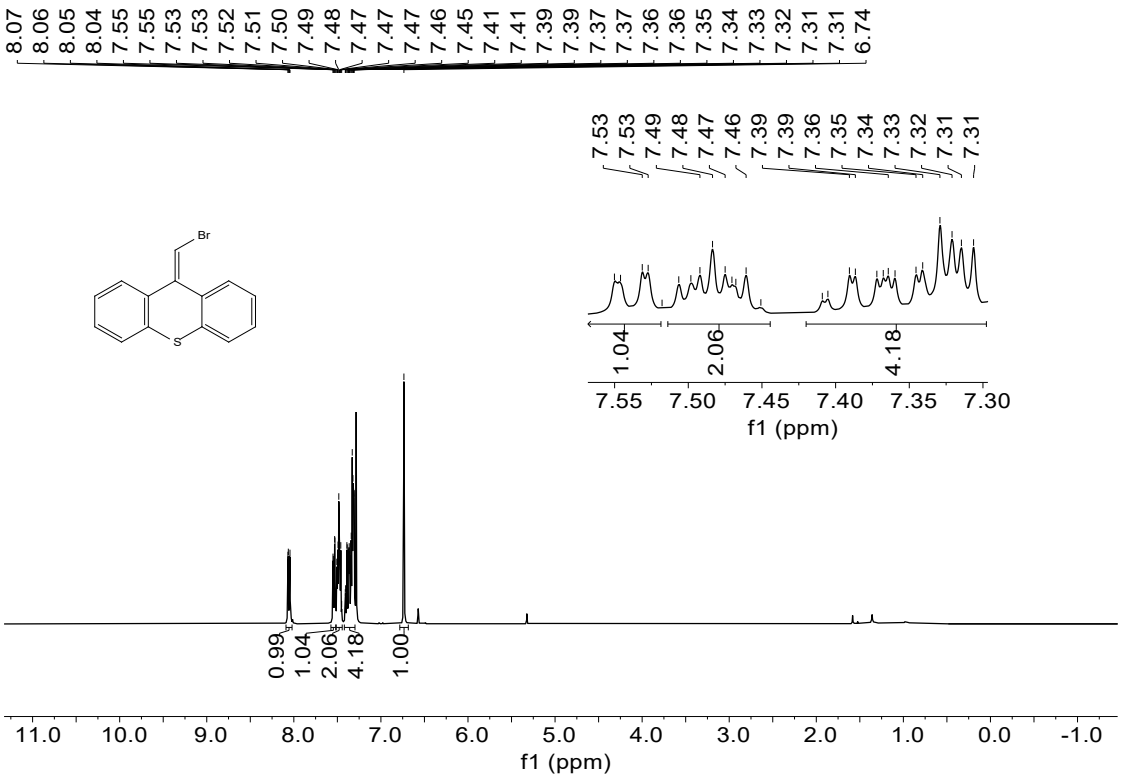

^{13}C NMR (101MHz, Chloroform-*d*) of compound **2**:

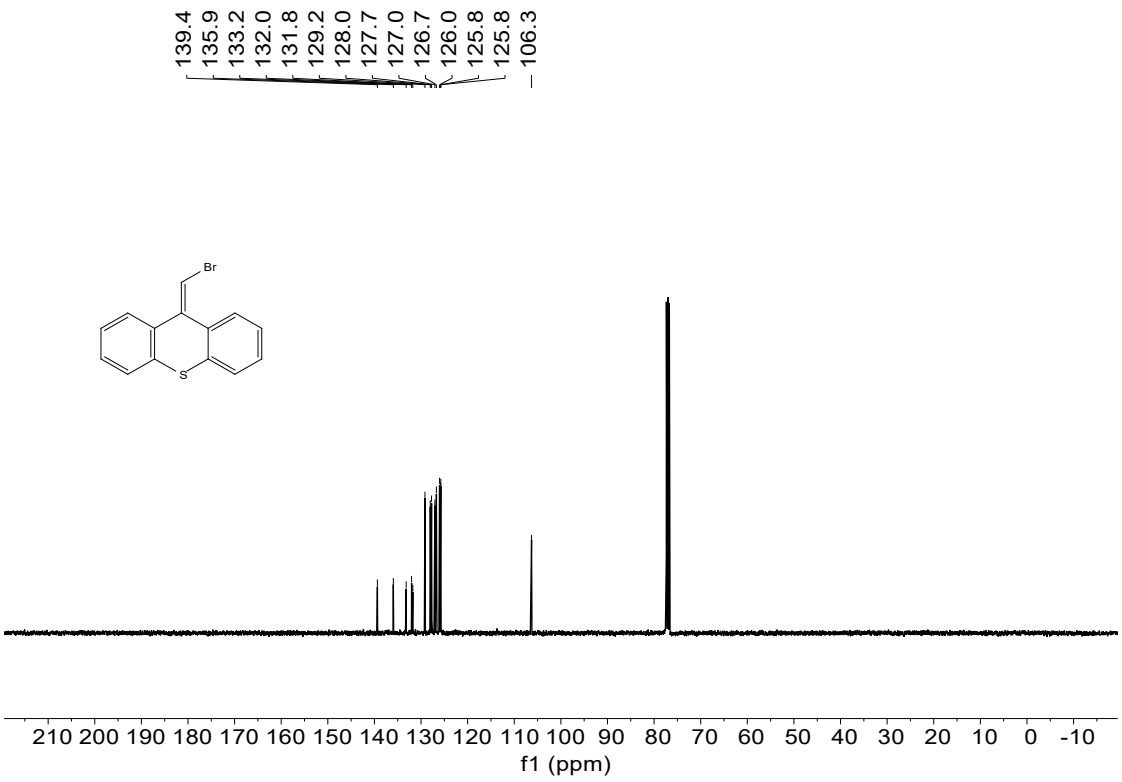

^{1}H NMR (400 MHz, Chloroform-*d*) of compound **TXENE**:

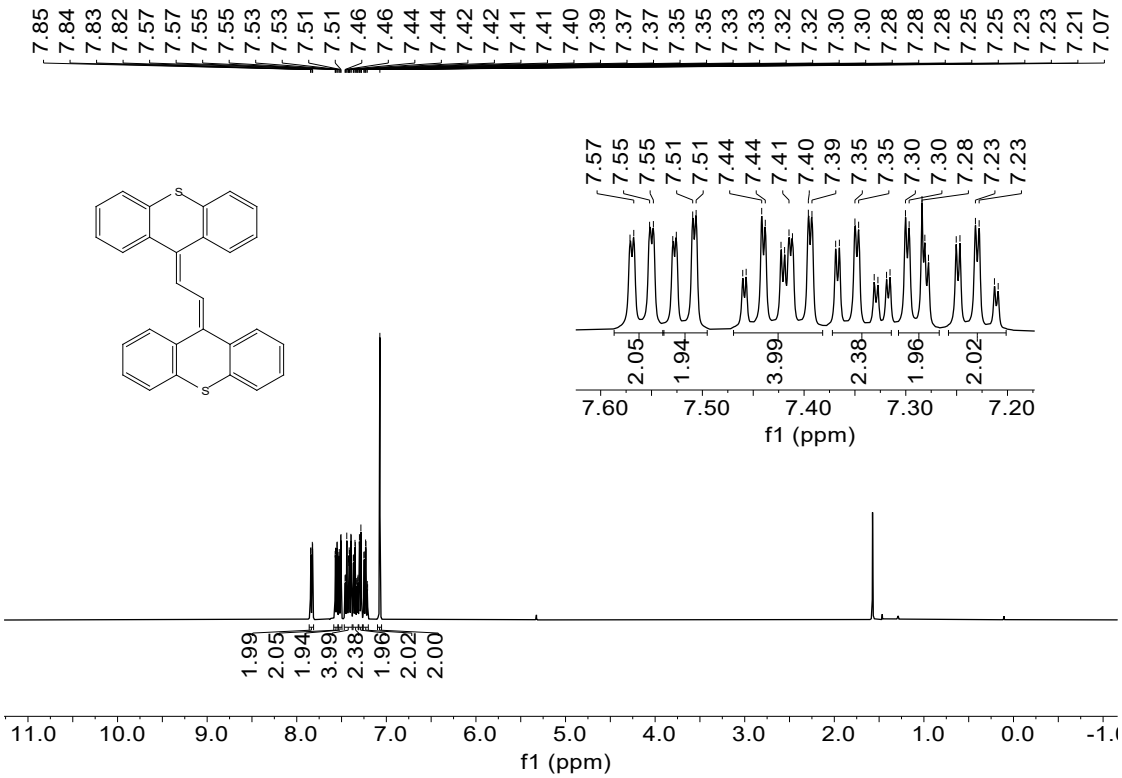

^{13}C NMR (101 MHz, Chloroform-*d*) of compound **TXENE**:

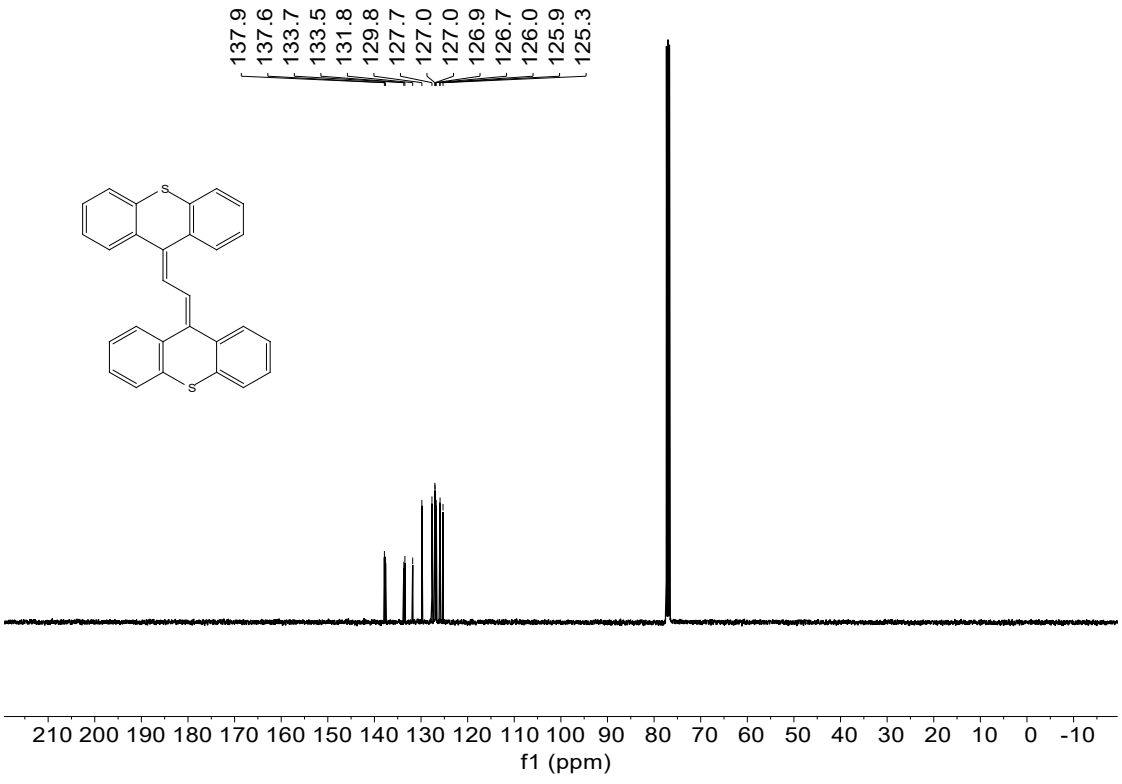

C. **Photophysical properties:**

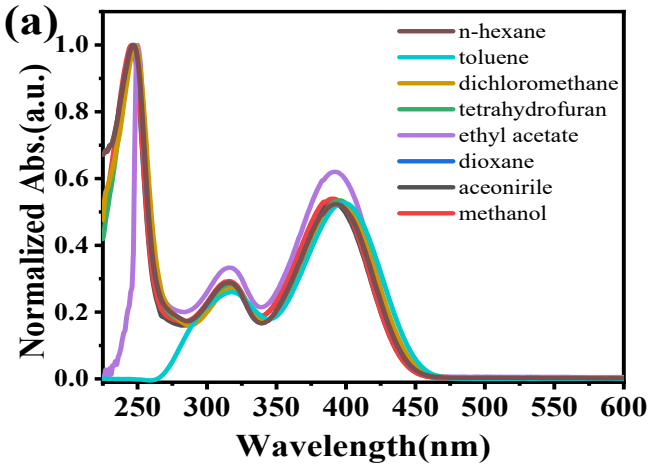

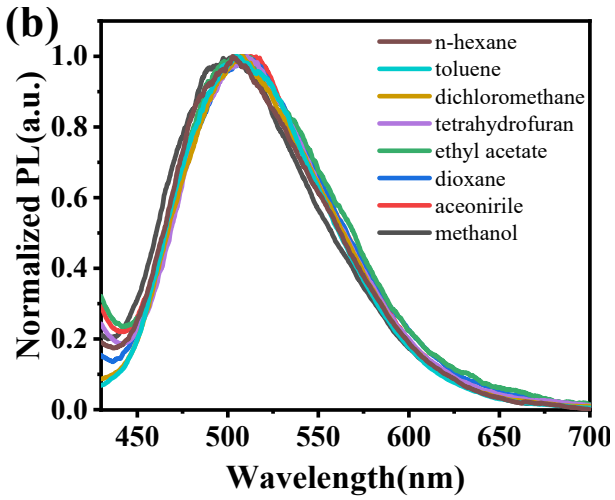

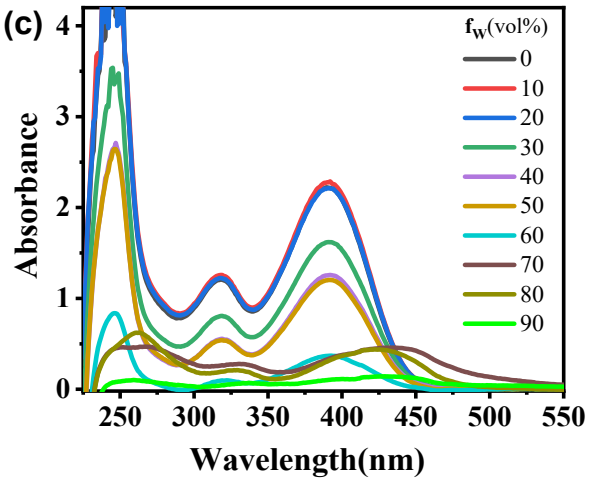

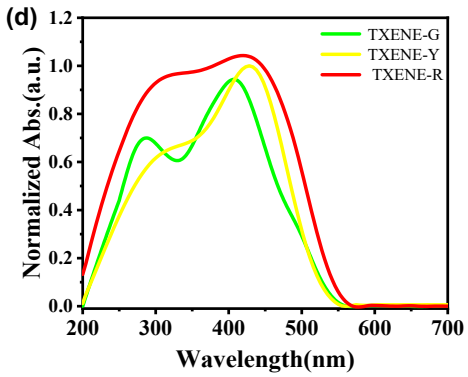

Figure S1. (a) UV-Vis absorption spectra; (b) PL emission spectra of TXENE in different solvents; (c) UV-Vis absorption spectra of TXENE in CH_3CN/H_2O mixtures (solution concentration is 5.0×10^{-5}M) (d) UV-Vis absorption spectra of TXENE-G, -Y and -R.

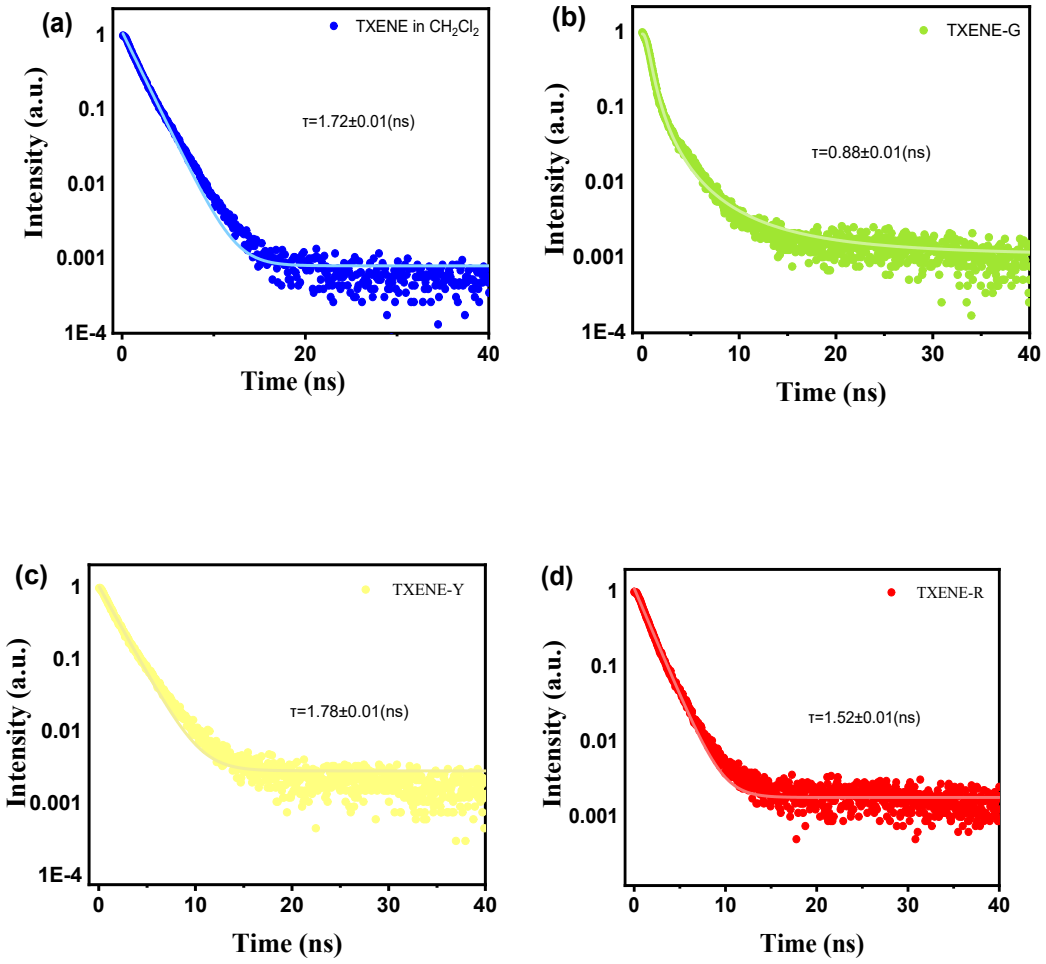

Figure S2. Photoluminescence lifetime of (a) TXENE solution; (b) TXENE-G; (c) TXENE-Y and (d) TXENE-R polymorphism under N_2 atmosphere (the solid line corresponds to the fitting result).

Table S1. Absorption and PL emission peaks of compounds TXENE in different solvents.

Medium	λ_{abs}[nm][a]	λ_{em}[nm]	Stokes shift[nm]	ϕ_F(%)[b]
n-hexane	395	503	108	0.08
toluene	398	505	107	0.17
dichloromethane	399	509	110	0.16
tetrahydrofuran	397	512	115	0.18
ethyl acetate	392	508	116	0.10
dioxane	393	511	118	0.06
acetonitrile	393	516	123	0.14
methanol	391	502	111	0.08

a. Absorption maximum in different solvents. b. Quantum yield in non-doped film estimated by integrating sphere.

Table S2. PL data of TXENE in DCM solution and in TXENE-G, -Y and -R solid states: PL maxima $\lambda_{em,}$ quantum yield Φ_F and intensity-averaged lifetime τ; radiative and nonradiative rates are obtained via $k_r = \Phi_F/\tau_F$ and $k_{nr} = (1-\Phi_F)/\tau_F$.

Entry	λ_{em} [nm]	Φ_F	τ_F [ns]	k_r [ns^{-1}]	k_{nr} [ns^{-1}]
DCM[a]	502	0.002	1.72	0.001	0.580
TXENE-G	495	0.154	0.88	0.175	0.961
TXENE-Y	537	0.295	1.78	0.166	0.396
TXENE-R	602	0.081	1.52	0.053	0.604

a. Concentration of 5×10^{-5} M.

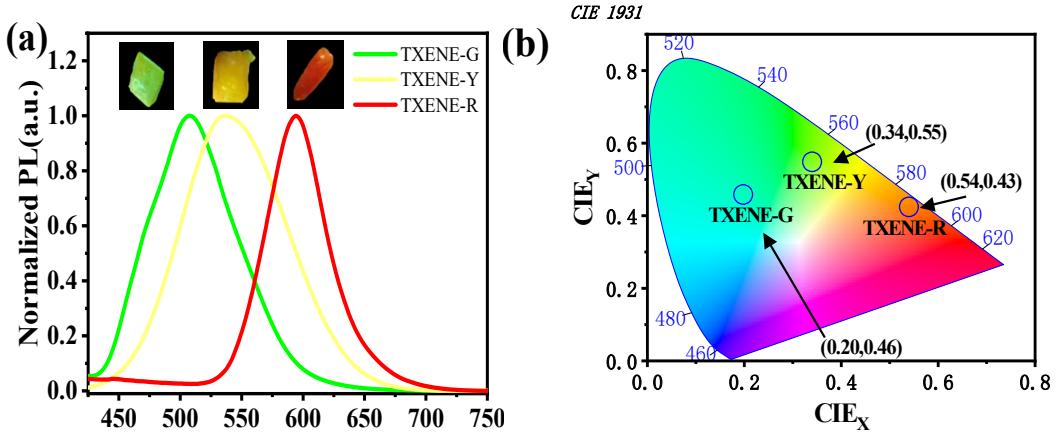

Figure S3. (a) PL spectra of TXENE in different aggregation states, inset shows the digital fluorescence images of crystals at 365 nm. (b) Calculated CIE coordinates according to the CIE 1931 chromaticity in different aggregation states of TXENE.

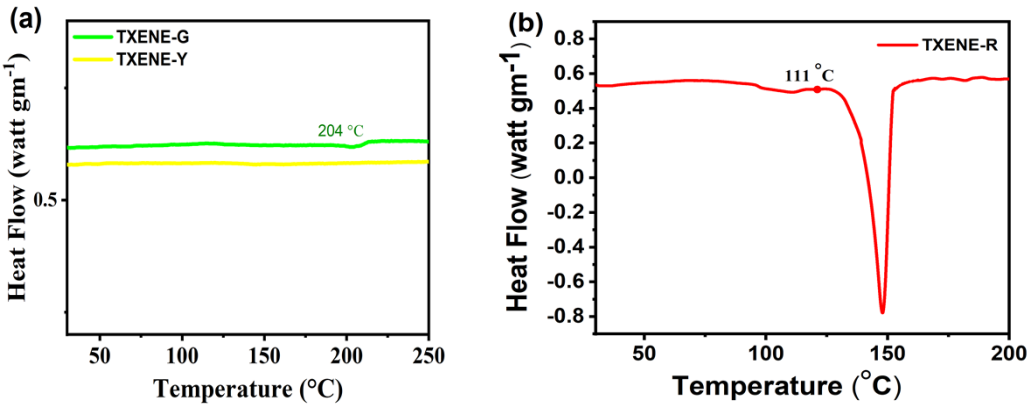

Figure S4. (a) DSC curve of TXENE-G and -Y. (b) DSC curve of TXENE-R.

D. Crystal structures and crystal data:

Crystal Data

Table S3. Crystal data and structure refinement for TXENE-G, TXENE-Y and TXENE-R.

Parameter	TXENE-G	TXENE-Y	TXENE-R
Empirical formula	$C_{28}H_{18}S_2$	$C_{28}H_{18}S_2$	$C_{56}H_{36}S_4$
CCDC number	2256586	2256585	2256584
Formula weight	418.54	418.54	837.09
Temperature/K	150.0	150.0	150.0

Crystal system	monoclinic	monoclinic	triclinic
Space group	$P2_{1/c}$	$P2_{1/c}$	P_{-1}
a/ Å	9.805(3)	9.810(2)	7.8616(9)
b/ Å	7.752(2)	7.7548(18)	11.3170(16)
c/ Å	13.324(3)	13.337(3)	12.3543(14)
α/°	90	90	85.065(6)
β/°	99.924(8)	99.872(7)	86.137(4)
γ/°	90	90	69.722(4)
Volume/ $Å^3$	997.5(4)	999.6(4)	1026.4(2)
Z	2	2	1
$\rho_{calc}g/cm^3$	1.393	1.391	1.354
μ/mm^{-1}	0.280	0.280	1.598
F(000)	436.0	436.0	436.0
Crystal size/mm^3	0.2×0.18×0.10	0.23×0.18×0.14	0.23×0.12×0.02
Radiation	MoKa (λ=0.71073)	MoKa (λ=0.71073)	GaKa (λ=1.3413)
2Θrange for data collection/°	4.218 to 55.068	4.214 to 52.728	6.252 to 99.302
Index ranges	-12≤h≤12, -10≤k≤9, -17≤l≤13	-12≤h≤12, -8≤k≤9, -16≤l≤16	-8≤h≤8, -10≤k≤12, -13≤l≤14
Reflections collected	8914	8357	6489
Independent reflections	2269 [Rint=0.0425, Rsigma=0.0400]	2046 [Rint=0.0479, Rsigma=0.0392]	2965 [Rint=0.0481, Rsigma=0.0573]
Data/restraints/parameters	2269/0/136	2046/0/136	2965/0/271
Goodness-of-fit on F^2	1.027	1.061	1.064
Final R indices [I>2sigma(I)]	R_1 = 0.0472, wR_2=0.1208	R_1 = 0.0462, wR_2=0.0902	R_1 = 0.0466, wR_2=0.1239
Final R indexes [all data]	R_1 = 0.0682, wR_2=0.1374	R_1 = 0.0693, wR_2=0.1023	R_1 = 0.0551, wR_2=0.1305
Largest diff. peak and hole	0.35/-0.32	0.22/-0.25	0.38/-0.43

Crystal structures

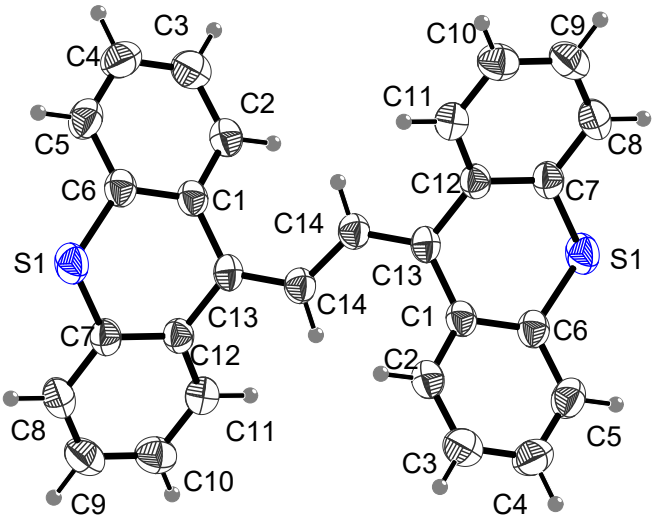

Figure S4. Single crystal structure of TXENE-G.

Table S4. Atomic coordinates and equivalent isotropic atomic displacement parameters (Å^2) of TXENE-G. U(eq) is defined as one third of the trace of the orthogonalized U_{ij} tensor.

Atom	***x***	***y***	***z***	**U(eq)**
C1	0.8428(19)	0.6803(3)	0.6125(16)	0.0374(4)
C2	0.8786(2)	0.8382(3)	0.5728(18)	0.0431(5)
C3	0.8810(2)	0.9879(3)	0.6280(2)	0.0514(6)
C4	0.8488(3)	0.9852(3)	0.7255(2)	0.0540(6)
C5	0.8086(2)	0.8336(3)	0.7652(18)	0.0492(5)
C6	0.8038(2)	0.6823(3)	0.7088(16)	0.0405(5)
C7	0.6613(2)	0.3924(3)	0.6478(16)	0.0397(5)
C8	0.5466(2)	0.2883(3)	0.6522(19)	0.0473(5)
C9	0.4802(2)	0.2068(3)	0.5658(2)	0.0528(6)
C10	0.5248(2)	0.2307(3)	0.4739(2)	0.0518(6)
C11	0.6390(2)	0.3316(3)	0.4693(17)	0.0440(5)
C12	0.7112(2)	0.4128(2)	0.5567(16)	0.0369(4)
C13	0.8361(2)	0.5178(2)	0.5538(15)	0.0360(4)
C14	0.9346(2)	0.4600(3)	0.5024(16)	0.0388(5)
S1	0.7451(6)	0.4922(8)	0.7603(4)	0.0501(2)

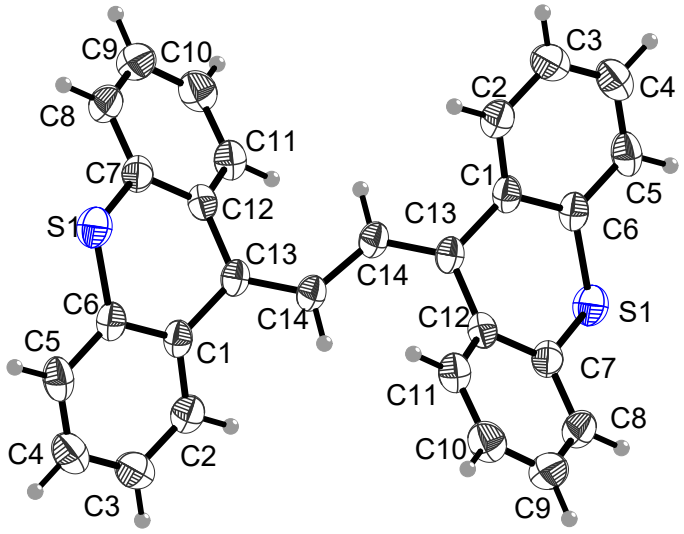

Figure S5. Single crystal structure of TXENE-Y.

Table S5. Atomic coordinates and equivalent isotropic atomic displacement parameters (Å^2) of TXENE-Y. U(eq) is defined as one third of the trace of the orthogonalized U_{ij} tensor.

Atom	*x*	*y*	*z*	U(eq)
C1	0.2888(2)	0.4126(3)	0.4434(16)	0.0344(5)
C2	0.3610(2)	0.3319(3)	0.5302(17)	0.0418(5)
C3	0.4748(2)	0.2306(3)	0.5259(19)	0.0486(6)
C4	0.5202(2)	0.2067(3)	0.4343(2)	0.0505(6)
C5	0.4533(2)	0.2879(3)	0.3479(19)	0.0457(6)
C6	0.3389(2)	0.3924(3)	0.3520(16)	0.0368(5)
C7	0.1963(2)	0.6824(3)	0.2909(16)	0.0382(5)
C8	0.1913(2)	0.8337(3)	0.2352(18)	0.0472(6)
C9	0.1509(3)	0.9857(4)	0.2745(2)	0.0528(7)
C10	0.1189(2)	0.9880(3)	0.3717(19)	0.0492(6)
C11	0.1217(2)	0.8381(3)	0.4268(18)	0.0418(6)
C12	0.1569(2)	0.6806(3)	0.3873(16)	0.0353(5)
C13	0.1638(2)	0.5173(3)	0.4457(15)	0.0340(5)
C14	0.0652(2)	0.4600(3)	0.4975(15)	0.0360(5)
S1	0.2548(6)	0.4922(9)	0.2396(4)	0.0479(2)

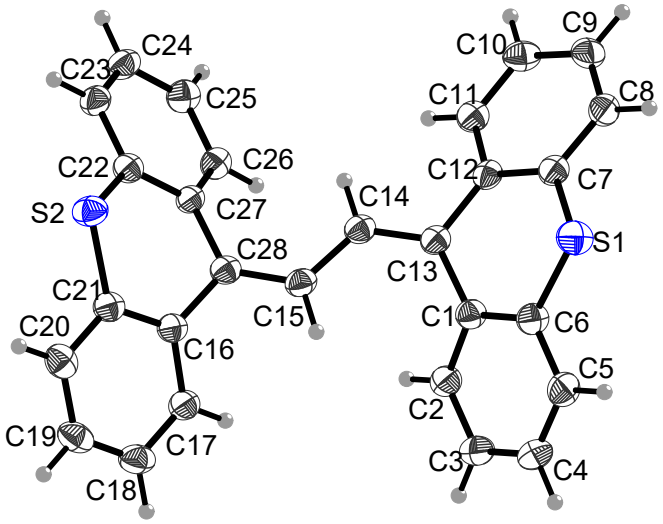

Figure S6. Single crystal structure of TXENE-R.

Table S6. Atomic coordinates and equivalent isotropic atomic displacement parameters (Å^2) of TXENE-R. U(eq) is defined as one third of the trace of the orthogonalized U_{ij} tensor.

Atom	*x*	*y*	*z*	U(eq)
C1	0.2759(3)	0.2050(2)	0.5755(18)	0.0302(5)
C2	0.1425(3)	0.1532(2)	0.5589(19)	0.0345(6)
C3	0.1453(4)	0.0388(2)	0.6101(2)	0.0418(6)
C4	0.2829(4)	-0.0265(2)	0.6808 (2)	0.0423(7)
C5	0.4108(3)	0.0247(2)	0.7031(2)	0.0374(6)
C6	0.4065(3)	0.1415(2)	0.6518(19)	0.0324(5)
C7	0.4485(3)	0.3682(2)	0.6642(18)	0.0304(5)
C8	0.4893(3)	0.4513(2)	0.7270(19)	0.0347(6)
C9	0.4083(3)	0.5802(2)	0.7065(19)	0.0359(6)
C10	0.2872(3)	0.6270 (2)	0.6233(2)	0.0365(6)
C11	0.2449(3)	0.5447(2)	0.5626(18)	0.0319(5)
C12	0.3244(3)	0.4138(2)	0.5812(17)	0.0278(5)
C13	0.2776(3)	0.3254(2)	0.5169(17)	0.0272(5)
C14	0.2427(3)	0.3557(2)	0.4101(18)	0.0288(5)
C15	0.2191(3)	0.2763(2)	0.3321(18)	0.0298(5)
C16	0.1947(3)	0.2074(2)	0.1528(18)	0.0281(5)
C17	0.1138(3)	0.1169(2)	0.1853(19)	0.0332(6)
C18	0.1295(3)	0.0192(2)	0.1207(2)	0.0380(6)
C19	0.2231(3)	0.0116(2)	0.0206(2)	0.0368(6)
C20	0.2987(3)	0.1022(2)	-0.0149(2)	0.0346(6)
C21	0.2848(3)	0.1998 (2)	0.0502(19)	0.0298(5)
C22	0.2507(3)	0.4441(2)	0.0682(18)	0.0293(5)
C23	0.2311(3)	0.5627(2)	0.0165(19)	0.0319(6)

Atom	*x*	*y*	*z*	U(eq)
C24	0.1236(3)	0.6709(2)	0.0646(19)	0.0349(6)
C25	0.0306(3)	0.6623(2)	0.1632(19)	0.0344(6)
C26	0.0495(3)	0.5446(2)	0.2146(18)	0.0306(5)
C27	0.1638(3)	0.4339(2)	0.1697(17)	0.0262(5)
C28	0.1910(3)	0.3065(2)	0.2248(18)	0.0280(5)
S1	0.5681(8)	0.2048(6)	0.6888(5)	0.0401(2)
S2	0.3922(8)	0.3090(5)	0.0029(5)	0.0354 (2)

E. Theroetical Study:

Density functional theory (DFT) computations on several molecular properties were listed in Table S6. These two orbitals are involved in the emission process as shown by time dependent DFT calculations, and the computational HOMO–LUMO gaps along the three species show the same trend with experimental fluorescent wavelengths.

Table S7: Properties of the three species. Energies in eV.

Species	HOMO	LUMO	HOMO-LUMO gap	S1
TXENE-G	-5.45	-1.98	3.47	3.08
TXENE-Y	-5.44	-2.04	3.40	3.03
TXENE-R	-5.26	-2.09	3.17	2.87
TXENE-G[a]	-5.35	-2.05	3.30	3.00
TXENE-Y[a]	-5.35	-2.07	3.28	2.98
TXENE-R[a]	-5.23	-2.05	3.18	2.87

[a] calculation based on two monomers with nearest shortest perpendicular π–π interactions.

Table S8. The optimised coordinates of transition states for TXENE-Y to TXENE-R.

Atom	*x*	*y*	*z*
C1	-4.6411	3.2670	0.8170
C2	-5.0830	1.9536	0.8660
C3	-4.1910	0.8904	0.6666
C4	-2.8169	1.1074	0.4321
C5	-2.4172	2.4606	0.3415
C6	-3.2955	3.5161	0.5379
C7	-2.3597	-1.3369	-0.1849
C8	-3.7311	-1.6760	-0.1300

C9	-4.2198	-2.8714	-0.6717
C10	-3.3688	-3.7544	-1.3222
C11	-2.0236	-3.4122	-1.4656
C12	-1.5489	-2.2187	-0.9385
C13	1.9201	-0.2132	-0.028
C14	3.0167	-1.1622	0.2476
C15	2.2904	1.1039	-0.5796
C16	2.8563	-2.5452	0.0518
C17	4.2636	-0.7068	0.7194
C18	3.4717	1.7539	-0.1658
C19	1.4982	1.7444	-1.5512
C20	3.8713	-3.4445	0.3580
C21	5.2893	-1.6091	1.0212
C22	3.7997	3.0227	-0.6543
C23	1.8210	3.0080	-2.0349
C24	5.0910	-2.9760	0.8523
C25	2.9685	3.6565	-1.5736
C26	-1.8445	-0.0102	0.2426
C27	-0.5117	0.3069	0.1800
C28	0.6263	-0.5711	0.2270
H1	-5.2800	-3.0919	-0.5867
H2	-5.3388	4.0846	0.9707
H3	-6.1316	1.7337	1.0448
H4	-1.3928	2.7073	0.0937
H5	-2.9293	4.5356	0.4621
H6	-3.7571	-4.6774	-1.7423
H7	-1.3488	-4.0556	-2.0226
H8	-0.5300	-1.9369	-1.1627
H9	0.6249	1.2273	-1.9336

H10	6.2424	-1.2327	1.3809
H11	4.7148	3.5027	-0.3202
H12	1.1868	3.4783	-2.7804
H13	5.8926	-3.6703	1.0863
H14	3.2319	4.6411	-1.9486
H15	1.9197	-2.9112	-0.3575
H16	3.7167	-4.5076	0.1995
H17	-0.2417	1.3492	0.2825
H18	0.4608	-1.5733	0.6108
S1	-4.8989	-0.7244	0.7936
S2	4.5596	1.0180	1.0292

F. References:

[1] O. V. Dolomanov, L. J. Bourhis, R. J. Gildea, J. A. K. Howard, H. Puschmann, *J. Appl. Crystallogr.* **2009**, 42, 339-341.

[2] G. M. Sheldrick, *Acta Crystallogr. Sect. A Found. Adv*. **2015**, 71, 3-8.

[3] T. H. Jepsen, M. Larsen, M. Jørgensen, M. B. Nielsen, *Synlett.* **2012**, 23, 418-422.

[4] G. Zhang, R. Bai, C. Li, C. Feng, G. Lin, *Tetrahedron.,* **2019**, 75, 1658-1662.